Characterizing the Optical Fingerprint of Duodenal Gastrinoma Using Quantitative Multi-Photon Autofluorescence Microscopy

Thomas G. Knapp[1], Suzann Duan[2], Juanita L. Merchant[2], Travis W. Sawyer[1,2,3]

Department of Biomedical Engineering,[1] College of Medicine,[2] and College of Optical Sciences,[3] University of Arizona

Biomedical Optics & Optical Measurement

THE UNIVERSITY OF ARIZONA

Background and Motivation

Duodenal gastrinoma tumors (DGasts) secrete the hormone gastrin which results in the over-production of stomach acid, a condition termed **Zollinger-Ellison Syndrome (ZES)**. ZES symptomology includes chronic diarrhea, stomach ulcers, tissue adhesions with increased risk of rupture, and malabsorption. **DGasts** typically develop as small, diffuse, lesions within the submucosa of the proximal small intestine (**Figure 1**). [1]

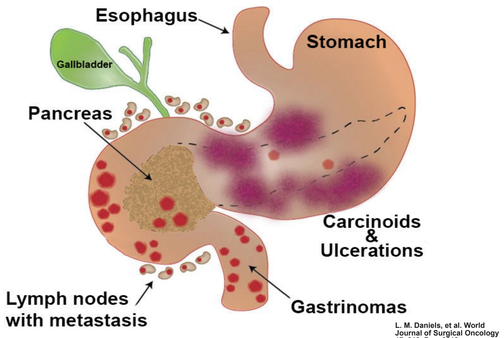

Figure 1:
Illustration of gastrinoma development and spread, showing the multifocal nature of the tumor and gastric damage secondary to acid hypersection.

Difficult resection of **DGasts** shifts the focus of treatment towards management of symptoms (e.g. PPI to reduce acid production), which does not mitigate the potential for tumor metastasis. Aggressive surgical resection, such as the Whipple procedure (**Figure 2**) is often recommended for patients at high-risk for spread of the cancer. [1]

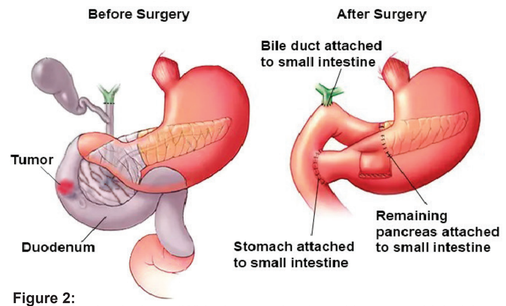

Figure 2:
Pancreaticoduodectomy (Whipple procedure) used to remove high-risk lesions within the region of the duodenum and pancreas.

Hypothesis

Differences in the composition between DGasts and normal duodenal tissue will provide contrast with endogenous fluorescence optical imaging, laying the ground work for augmented diagnostic and targeted resection tools.

Methods

Endogenous fluorescence was measured in formalin-fixed and paraffinized (FFPE) **Dgast** samples from 12 patients using two-photon microscopy (Zeiss LSM 880 NLO microscope).† Excitation wavelengths and detection bands (**Figure 3**) were chosen to collect fluorescence from molecules related to common markers of cancer:

- NADH: excitation: 700 nm; emission: 425 - 465 nm
- FAD: excitation: 925 nm; emission: 465 - 600 nm
- lipofuscin: excitation: 830 nm; emission: 550 - 600 nm
- porphyrin: excitation: 800 nm; emission: 590 - 625 nm

The **optical redox ratio** is a measure of tissue metabolic state determined by the ratio of **NADH** to **FAD** fluorescence.[2,3] **Second-harmonic generation** (**SHG**) is a light-scattering phenomena that is elicited by collagen structures. **SHG** was measured with 880 nm excitation and a 430 - 450 nm detection band.

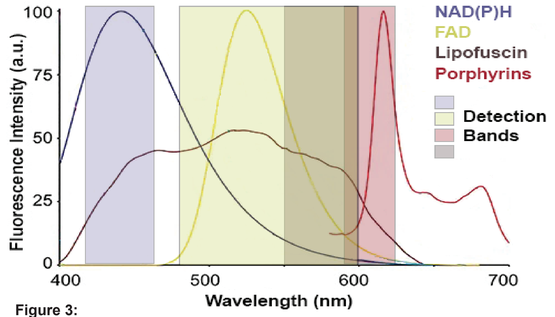

Figure 3:
Fluorescence spectra of endogenous fluorophores used for image contrast in this study. Note, fluorescence emission occurs at varying excitation light wavelengths, allowing for overlapping detection bands without severe fluorescence crosstalk.

Two-photon microscopy images and tissue stains of DGast samples

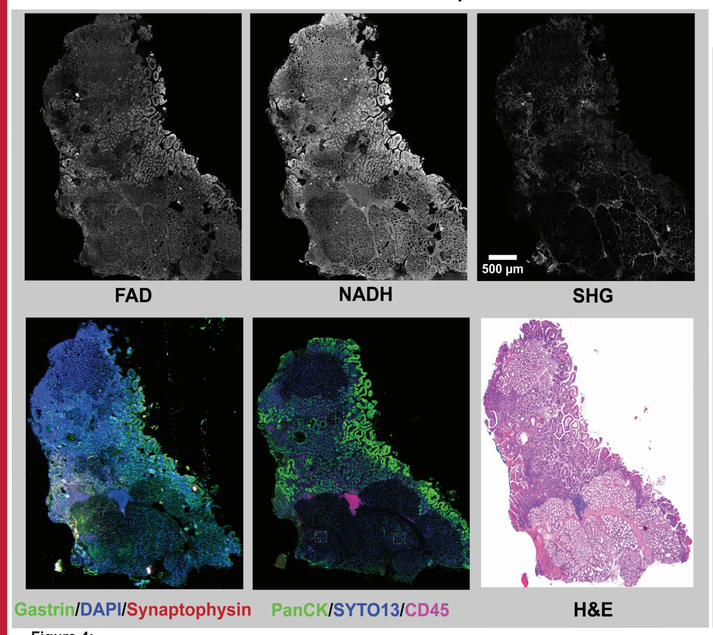

Figure 4:
Comparison of three of the imaging channels captured with two-photon microscopy and three different types of staining used to validate tissue types. **Gastrin/Synaptophysin** are specific for gastrin-producing cells and neuroendocrine tumors, respectively. **PanCK/SYTO13/CD45** are specific for epithelium, nucleic acids, and immune cells, respectively

Regions of interest (ROIs) used for measurement of relative fluorescence intensity between tissue types

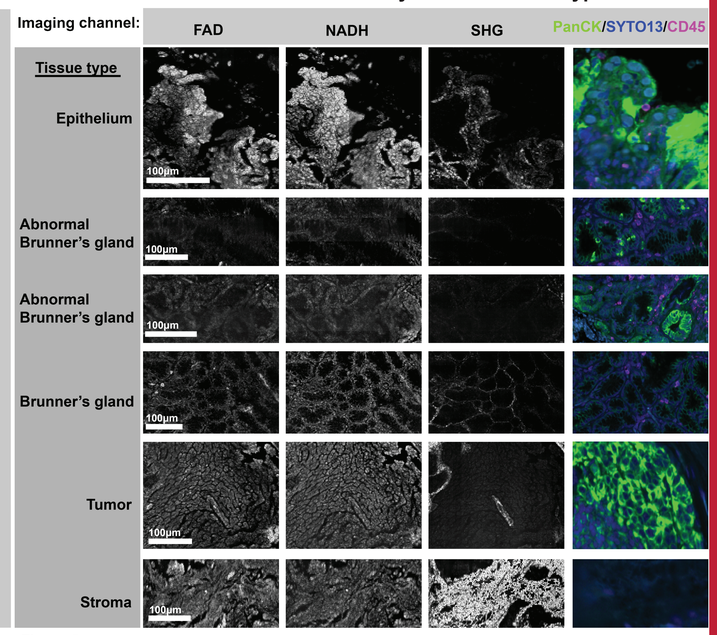

Figure 5:
ROIs of different tissue classifications used to measure and compare relative fluorescence intensities. Note the morphologic changes that occur between the **normal/abnormal Brunner's glands** (**BGs**) and **tumor**, which are thought to originate from cells within **BGs**. The immunostained images (shown on far right) were used to distinguish between sites of **normal/abnormal glands**.

Results

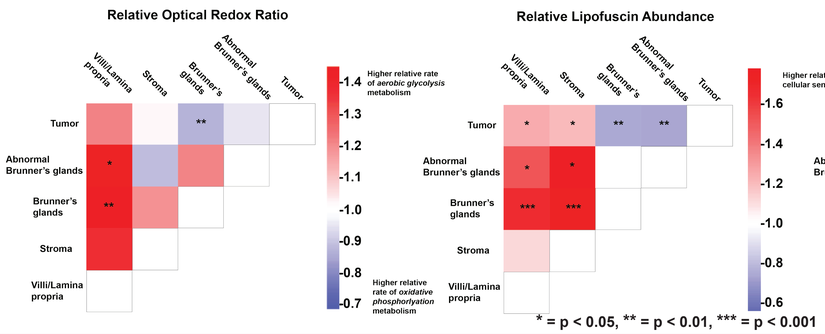

Figure 6:
Heat matrices showing comparisons of fluorescence intensities measured between the different tissue type within each sample. Matrices are calculated, and can be read, by **dividng the column classification by the row**. Higher values suggest a greater amount of the fluorophore existing within the tissue type, or in the case of the **optical redox ratio**, a variation in the metabolic state between the tissue types. ROIs were thresholded to remove fluorescence cross-talk and background noise. Comparisons between tissue were only made from within-sample ROIs to control for variations in acquisitions and samples.

Conclusion

Significant differences in signal intensity of endogenous fluorophores is measurable in FFPE samples of **DGast** using two-photon microscopy. **This suggests that endogenous fluorescence can be used as a label-free approach for distinguishing DGasts from healthy tissue due to differences in the relative abundances of fluorophores between tissue types.** Specifically, our findings show fluorescence signals related to tissue metabolism, cell senescence, and local blood concentration[4] (**Figure 6**) have significantly different values when measured in **DGast tumors** and **normal tissue of the duodenum**.

Future Directions

Current efforts are focused on image texture analysis using **Haralick feature extraction** [6] of the fluorescence and SHG images, which provides statistics on the spatial relationship of pixel gray-level values. Discriminant analyses (Example **Figure 7**) from each of the five image channels will provide insight into the type and number of features required for adequate **discrimination of the DGast tumors from their surrounding environment**. This information will inform further work in the development of imaging systems used for in-vivo detection of **DGasts** and other neuroendocrine tumors.

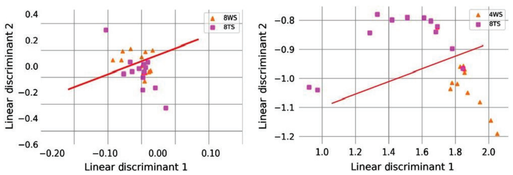

Figure 7:
Two sets of linear discriminant analysis done in work by Sawyer et al [5], each using two linear discriminants derived from Haralick feature extraction of SHG and multi-photon fluorescence images of murine ovaries.

Acknowledgements

Special thanks to the Marley Imaging Core supervisor, Patty Jansma, for her assistance with the multi-photon microscope, and to the members of the B.O.O.M. and Merchant laboratories for their aid in this ongoing project.
Financial support for this work was provided by core facility grant CA-CFPP April 2021 ICMarley-3502090 and NIH grant GM132008.

References

[1] Norton, J. A. (2005). **Surgical treatment and prognosis of gastrinoma**. Best Practice & Research Clinical Gastroenterology, 19(5), 799–805. https://doi.org/10.1016/J.BPG.2005.05.003
[2] Zipfel, W. R., Williams, R. M., Christie, R., Nikitin, A. Y., Hyman, B. T., & Webb, W. W. (2003). **Live Tissue Intrinsic Emission Microscopy Using Multiphoton-Excited Native Fluorescence and Second Harmonic Generation**. Proceedings of the National Academy of Sciences of the United States of America, 100(12), 7075–7080. http://www.jstor.org/stable/3139434
[3] Walsh AJ, Cook RS, Sanders ME, et al. **Quantitative optical imaging of primary tumor organoid metabolism predicts drug response in breast cancer.** Cancer Res. 2014;74(18):5184-5194. doi:10.1158/0008-5472.-CAN-14-0663
[4]Nishida, K., Tojo, T., Kondo, T. et al. Evaluation of the correlation between porphyrin accumulation in cancer cells and functional positions for application as a drug carrier. Sci Rep 11, 2046 (2021). https://-doi.org/10.1038/s41598-021-81725-3
[5]Sawyer TW, Koevary JW, Rice FPS, et al. **Quantification of multiphoton and fluorescence images of reproductive tissues from a mouse ovarian cancer model shows promise for early disease detection.** J Biomed Opt. 2019;24(9):1-16. doi:10.1117/1.JBO.24.9.096010
[6]R. M. Haralick, K. Shanmugam and I. Dinstein, **"Textural Features for Image Classification,"** in IEEE Transactions on Systems, Man, and Cybernetics, vol. SMC-3, no. 6, pp. 610-621, Nov. 1973, doi: 10.1109/TSMC.1973.4309314.
† Imaging Core Marley, University of Arizona